Article

Not peer-reviewed version

EaSiCroM (Easy Simulation Crop Model): A Simplified Modelling Framework for Sustainable Irrigation Management and Crop Water Productivity

Pasquale Garofalo *, Luca Musti , Donato Impedovo , Michele Rinaldi , Francesco Ciavarella , Sergio Ruggieri

Posted Date: 16 March 2026

doi: 10.20944/preprints202603.1175.v1

Keywords: crop simulation model; decision support system; irrigation scheduling; sustainable agriculture; district-scale simulations

Article

EaSiCroM (Easy Simulation Crop Model): A Simplified Modelling Framework for Sustainable Irrigation Management and Crop Water Productivity

Pasquale Garofalo [1,*], Luca Musti [2], Donato Impedovo [2], Michele Rinaldi [3], Francesco Ciavarella [3] and Sergio Ruggieri [1]

[1] Council for Agricultural Research and Economics (CREA), Research Centre for Agriculture and Environment, 70125 Bari, Italy
[2] University of Bari Aldo Moro, Department of Computer Science, 70121 Bari, Italy
[3] Council for Agricultural Research and Economics (CREA), Research Centre for Cereal and Industrial Crops, 71121 Foggia, Italy
* Correspondence: pasquale.garofalo@crea.gov.it

Abstract

Crop simulation models and irrigation decision support systems (IDSS) are essential tools for improving water-use efficiency in agriculture, particularly in Mediterranean and semi-arid regions where water scarcity is a major constraint. However, many operational platforms are either too complex and data-demanding for widespread adoption or too simplified to adequately simulate crop responses to the combined effects of temperature, water stress, and elevated CO_2. This paper presents the Easy Simulator Crop Model (EaSiCroM), a modular, low-parameterisation decision support system designed to simulate daily crop growth, soil water dynamics, and irrigation requirements. EaSiCroM simulates canopy development through a beta-function-derived leaf area index (LAI) trajectory and Beer–Lambert canopy cover (CC), with growth progressively constrained by temperature (Tlim) and water stress (Kstress and KScc). Biomass accumulation is estimated through a water-productivity (WP) approach, optionally complemented by a radiation-use efficiency (RUE) pathway. A Michaelis–Menten sub-model accounts for the CO_2 fertilisation effect on WP and RUE. The soil water balance includes a two-stage bare-soil evaporation formulation and supports multiple irrigation triggering strategies. EaSiCroM is implemented as a Docker-containerised web application supporting single-crop, multi-plot, and near-real-time irrigation modes. The model requires a limited parameter set, operates at daily time steps, and integrates user-provided canopy observations (field or remote sensing) for adaptive irrigation scheduling. Its modular architecture and accessible interface make it suitable for both research and operational irrigation management in water-scarce agricultural systems.

Keywords: crop simulation model; decision support system; irrigation scheduling; sustainable agriculture; district-scale simulations

1. Introduction

Agriculture is the largest consumer of fresh water globally, accounting for approximately 70% of total withdrawals, and this proportion rises to over 80% in Mediterranean and semi-arid regions [1,2]. In Southern Europe, spring and summer crops depend almost entirely on irrigation because seasonal precipitation is scarce, irregularly distributed, and declining under ongoing climate change [3]. At the same time, urbanisation, industrial development, and environmental protection intensify competition for the same water resources, progressively reducing the agricultural share and driving irrigation water costs upward [4]. Italy alone accounts for nearly 50% of its national water withdrawals in agriculture, one of the highest rates in Europe [5].

 doi:10.20944/preprints202603.1175.v1

The stakes could not be higher: global food demand is expected to increase by 50–70% by 2050 [6], while climate projections consistently signal reductions of 20–45% in maize yields, 5–50% in wheat, and 20–30% in rice by 2100 under medium-to-high emission scenarios [7,8]. Against this backdrop, improving crop water-use efficiency – producing more food per unit of water – has become a central research and policy priority, explicitly enshrined in the United Nations Sustainable Development Goals 2 and 6 [9]. Achieving this goal requires tools that bridge the gap between agronomic knowledge and field-level decision making.

Irrigation decision support systems (IDSS) have long been recognised as effective instruments for translating that knowledge into actionable, site-specific recommendations [10,11]. At the mechanistically rich end, models such as DSSAT [12], APSIM [13], AquaCrop [14], CropSyst [15], and RZWQM [16] formalise the biophysical processes underlying soil water movement, root growth, photosynthesis, and phenological development. Platforms such as ADEAUMIS [17,18], MIRRIG [19], and FDSS [20] extend these approaches to farm- and district-scale management. The scientific rigour of these systems is not in question; yet their high parameterisation requirements, calibration complexity, and steep learning curves severely restrict their uptake outside specialised research contexts.

At the other extreme, simplified water balance models and empirical crop coefficient approaches [21] are operationally accessible but typically fail to simulate dynamic canopy development, represent multiple co-occurring stress factors, or integrate near-real-time field observations into ongoing simulations. A further limitation shared by many existing IDSSs is their static, single-period scheduling framework, which cannot readily assimilate user-provided observational data (e.g. remotely sensed vegetation indices or field measurements) to correct model trajectories during the growing season [22,23].

These considerations motivated the development of the Easy Simulator Crop Model (EaSiCroM), a modular, low-parameterisation decision support system that seeks a deliberate and principled balance between mechanistic realism and operational simplicity. EaSiCroM is grounded in three foundational design criteria: (i) parsimony – relying on a limited set of parameters with clear physiological interpretation, estimable from standard agronomic experiments or published literature; (ii) modularity and transparency – a hierarchically ordered architecture in which each process module receives inputs from the preceding one and feeds outputs to the next, enabling straightforward diagnosis of model behaviour and targeted calibration; and (iii) adaptability – supporting multiple irrigation triggering strategies, concurrent multi-plot simulations, CO_2 fertilisation effects, user-provided canopy observations canopy assimilation, and multiple ET_0 estimation methods when meteorological data are incomplete.

EaSiCroM builds on and substantially extends the empirical framework originally proposed for processing sunflower and biomass sorghum in a Mediterranean environment [24,25]. EaSiCroM extends and formalises this modelling line by incorporating a revised piecewise-linear temperature stress formulation, a two-stage soil evaporation model, a radiation-use efficiency co-limiting pathway, a Michaelis-Menten CO_2 fertilisation sub-model, user-provided canopy data assimilation, a precision real-time mode, and full deployment as a containerised web application. The primary objective of this paper is to provide a rigorous, equation-level description of EaSiCroM – its theoretical foundations, mathematical formulation, internal architecture, and key design decisions – so that the scientific community can evaluate, reproduce, and extend the framework. Applications to specific crops and experimental datasets, together with full model validation across Mediterranean environments, will be the subject of separate publications.

2. Model Description

2.1. General Architecture and Inputs

EaSiCroM operates at a daily time step and is structured as a directed sequence of computational modules, each building on the outputs of its predecessors. Three categories of inputs are required.

First, daily meteorological data: minimum, maximum, and mean temperature (°C); precipitation (mm); reference evapotranspiration ET_0 (mm); and, optionally, incoming solar radiation Rg (MJ m^{-2}). When ET_0 is not directly available, EaSiCroM estimates it internally using the Penman-Monteith equation [21] when wind speed, relative humidity, and radiation are provided; the Priestley-Taylor method when radiation and temperature are available; or the Blaney-Criddle empirical approach when only temperature data are given – a layered fallback strategy that substantially broadens the system's applicability in data-scarce contexts. Second, soil hydraulic properties: volumetric water content at field capacity (θFC) and permanent wilting point (θWP), root-zone depth, readily evaporable water (REW), and total evaporable water (TEW), calculated internally by EaSiCroM as:

$$TEW = (PAW\theta FC - 0.5 \cdot PAW\theta WP) \cdot Ze \quad (1)$$

where PAW is plant-available water and Ze is the evaporable top-soil depth. Third, crop-specific parameters describing thermal thresholds, canopy dynamics, water productivity, yield partitioning, and CO_2 response. The full daily computation sequence proceeds through the following successive steps, detailed in the following sections. Starting from daily weather inputs, the model first establishes the thermal environment by computing a temperature limiting factor (T_{lim}) and accumulating growing degree days. From these it derives the potential canopy trajectory through a beta-function LAI and Beer-Lambert canopy cover. The soil water balance is then updated with the previous day's fluxes, yielding the root-zone water content from which a soil-water availability indicator (Kstress) and its derived crop adaptive response (KScc) are computed. These stress quantities are applied to constrain canopy expansion, from which actual and stress-corrected transpiration are estimated. Daily biomass is then accumulated via the water-productivity and, optionally, radiation-use-efficiency pathways. Soil evaporation from the bare fraction completes the total crop evapotranspiration budget and finally yield formation and irrigation decisions are evaluated.

2.2. Temperature Limiting Factor and Thermal Time

The temperature limiting factor Tlim ∈ [0, 1] quantifies the daily degree to which ambient temperature permits plant growth. It is computed from the daily mean air temperature T_{mean} (°C) as:

$$Tlim = \begin{cases} 0 \quad if \quad T_{mean} < T_{base} \\ \frac{T_{mean}-T_{base}}{T_{opt}-T_{base}} \quad if \quad T_{base} \le T_{mean} \le T_{opt} \\ \frac{T_{max,crit}-T_{mean}}{T_{max,crit}-T_{opt}} \quad if \quad T_{opt} < T_{mean} \le T_{max,crit} \\ 0 \quad if \quad T_{mean} > T_{max,crit} \end{cases} \quad (2)$$

where T_{base} is the base temperature below which growth ceases, T_{opt} is the optimum temperature at which T_{lim} reaches unity, and $T_{max,crit}$ is the critical maximum temperature above which growth is fully suppressed. The function produces a triangular response curve: T_{lim} increases linearly from zero at T_{base} to unity at T_{opt}, then declines linearly back to zero at $T_{max,crit}$, consistent with the physiologically grounded temperature responses observed across a wide range of crop species [26]. Figure 1 illustrates the resulting T lim curve for a generic annual crop with example cardinal temperature values.

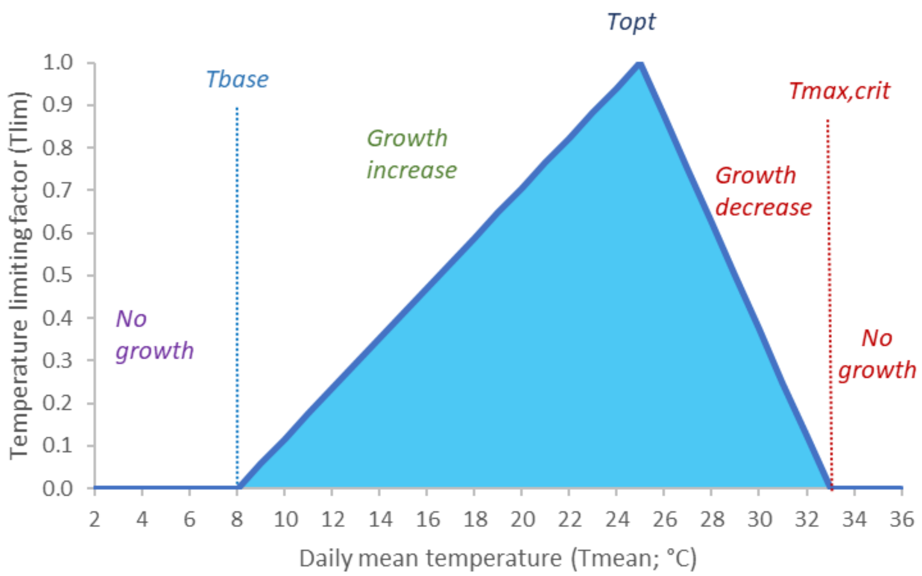

Figure 1. Temperature limiting factor T_{lim} as a function of daily mean temperature (T_{base} = 8°C, T_{opt} = 25°C, $T_{max,crit}$ = 33°C) as example values for a generic annual crop, simulated by EaSiCroM.

2.3. Potential Canopy Development

The potential (unstressed) leaf area index LAI ($m^2\ m^{-2}$) follows a beta function of GDD_{cum} [24,25]:

$$\mathrm{LAI} = LAI_{\max}\cdot\left(1+\frac{GDD_{end}\text{-}GDD_{cum}}{GDD_{end}\text{-}GDD_{\mathrm{LAI,max}}}\right)\cdot\left(\frac{GDD_{cum}}{GDD_{end}}\right)^{\left(\frac{GDD_{end}}{GDD_{end}\text{-}GDD_{\mathrm{LAI,max}}}\right)} \quad (3)$$

where LAI_{max} is the maximum leaf area index, $GDD_{LAI,max}$ the cumulated thermal time for the maximum active growth, and GDD_{end} the thermal time at beginning of canopy senescence. The beta function is mathematically well-behaved and unimodal; its three parameters correspond directly to measurable agronomic quantities, making calibration tractable even from limited datasets. The natural decline it produces beyond $GDD_{LAI,max}$ reflects the progressive senescence of leaves during ripening and grain filling, without requiring an explicit sub-stage formalism [27].

To account for the non-random distribution of leaves within the canopy – a phenomenon known as clumping – a correction factor CF is introduced:

$$CF = 0.75 + 0.25\cdot(1\text{-}e^{-0.35\cdot LAI}) \quad (4)$$

CF converges from 0.75 at sparse cover (strong clumping) towards 1 as LAI increases (random-equivalent distribution). Without this correction, the Beer-Lambert law systematically overestimates light interception and hence transpiration at low LAI, a bias with particular relevance during early crop establishment. The daily canopy cover fraction CC (dimensionless, 0–1) is then:

$$CC = 1\text{-}e^{-f_{cover}\cdot LAI\cdot CF} \quad (5)$$

where f_{cover} is the light extinction coefficient (typically 0.72 for broadleaf crops). CC represents the fraction of the soil surface shaded by the canopy and is the central variable linking canopy development to transpiration, soil evaporation, and biomass accumulation throughout the model. In Figure 2 is reported the potential canopy development of biomass sorghum with parameter values derived from [25].

The impact of the T_{mean} weather variable (and its effect on T_{lim} calculation) on potential canopy growth (see Equation 14) is shown in Figure 3.

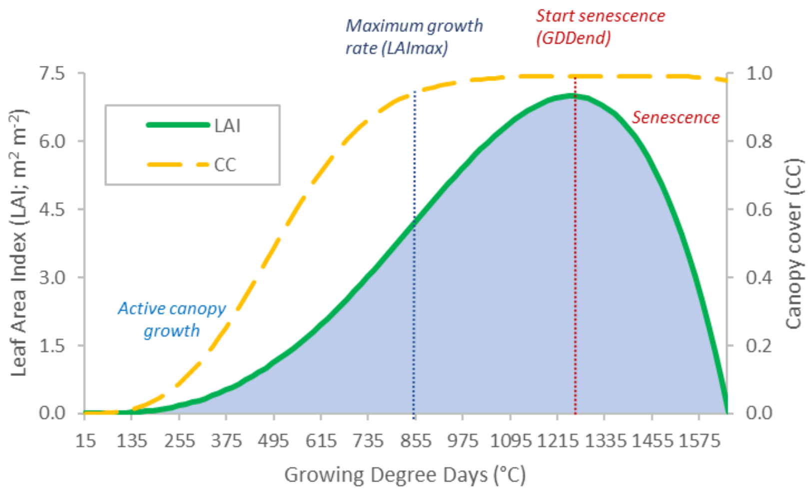

Figure 2. Potential leaf area index and canopy cover (LAI, CC) of biomass sorghum (details reported in Garofalo et al., 2020) as functions of cumulated growing degree days simulated by EaSiCroM.

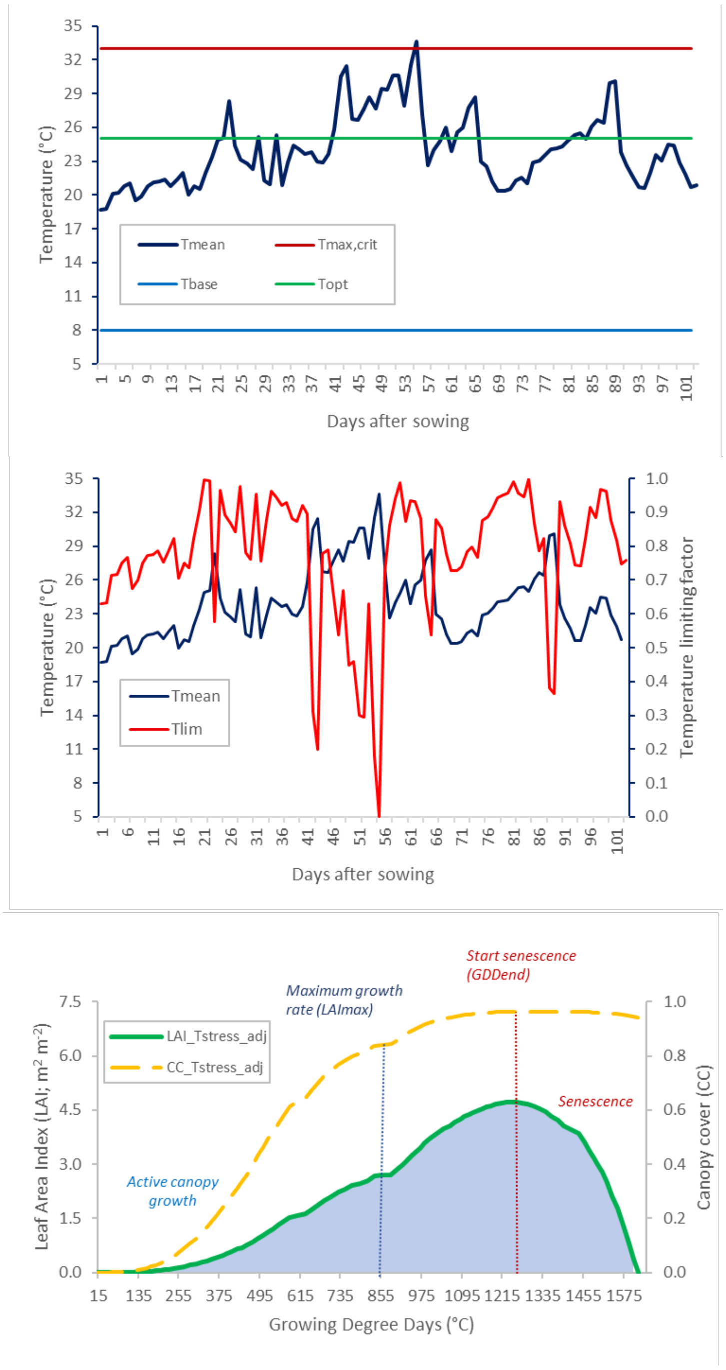

Figure 3. Effect of daily mean temperature (above) on the temperature limiting factor T_{lim} (middle) and on stress-adjusted canopy development for biomass.

2.4. Soil Water Balance

The soil water balance is maintained at daily resolution within the root zone. The total available water TAW_t (mm) is updated each day by subtracting crop water use and adding inputs from precipitation and irrigation:

$$TAW_t = AWC_{t-1} - (Tr_{adj,t-1} + TEr_{adj,t-1}) + P_{t-1} + IRR_{t-1} \quad (6)$$

where AWC_{t-1} is the available water content on the previous day (mm), Tr_{adj} is the stress-corrected transpiration (mm), E_{adj} the actual soil evaporation (mm), P precipitation (mm), and IRR applied irrigation (mm). On the first day of simulation, TAW is initialised to the user-specified or observed root-zone water content. Drainage from the root zone occurs whenever water exceeds field capacity:

$$Drainage_t = \max(AWC_t - \theta_{FC}, 0) \quad (7)$$

The available water content after drainage is:

$$AWC_t = TAW_t\text{-}Drainage_{t\text{-}1} \quad (8)$$

and Drainage$_t$ is:

$$Drainage_t = \max\,(AWC_t - \theta_{FC},\, 0) \quad (9)$$

A normalised water availability index AW_Δ ∈ [0, 1] is derived as:

$$AW\_\Delta = \frac{AWC\text{-}\theta_{\mathrm{WP,root}}}{\theta\Delta} \quad (10)$$

where θΔ = θFC,root − θWP,root is the total plant-available water capacity in the root zone. AW_Δ equals 0 at permanent wilting point and 1 at field capacity, serving as the dimensionless reference for both water stress and evaporation sub-models.

2.5. Water Stress Coefficients

EaSiCroM handles water stress through a two-stage cascade. First, it computes Kstress, a dimensionless indicator of soil-water availability derived directly from root-zone water content (Equation 11). Kstress acts as the primary stress trigger: it controls how much of the potential transpiration can be extracted from the soil and therefore directly enters the water balance. However, because crops are not passive recipients of water deficit — they actively respond by adjusting turgor, closing stomata, and reorienting growth — EaSiCroM then derives a second quantity, KScc, non-linearly from Kstress (Equation 12). KScc represents the adaptive canopy-expansion response of the crop to the water deficit signalled by Kstress: it modulates the rate of leaf-area expansion, reflecting the well-established physiological observation that cell elongation is more sensitive to water deficit than gas exchange [28,29].

Kstress ∈ [0, 1] is computed as a piecewise linear function of the available water content (AWC), proportional to the degree of root-zone filling between wilting point and field capacity:

$$\begin{cases} K_{stress} = 1 & \text{if } AWC \geq \Delta + \theta_{\mathrm{WP,root}} \\ K_{stress} = 0 & \text{if } AWC \leq \theta_{\mathrm{WP,root}} \\ & \text{otherwise} \\ K_{stress} = \dfrac{AWC\text{-}\theta_{\mathrm{WP,root}}}{\Delta} & \end{cases} \quad (11)$$

This proportional reduction in water uptake as the soil dries is consistent with evidence across many species and soils [14,30] and follows the FAO-56 framework [21]. KScc is then derived from Kstress via a non-linear transformation governed by a shape parameter α:

$$KS_{cc} = \frac{e^{K_{stress}\cdot\alpha}\text{-}1}{e^{\alpha}\text{-}1} \quad (12)$$

where α is a shape parameter. For $\alpha < 0$ the function is concave (Figure 4), meaning that canopy expansion is relatively tolerant of mild water deficits and only declines sharply as Kstress approaches zero – behaviour that reflects the osmotic adjustment and turgor maintenance mechanisms operative in many crops gradually developing drought [29].

The same Kstress that drives KScc also enters the soil water balance directly as the proportional reduction in transpired water, thus maintaining full consistency between canopy state and soil moisture accounting.

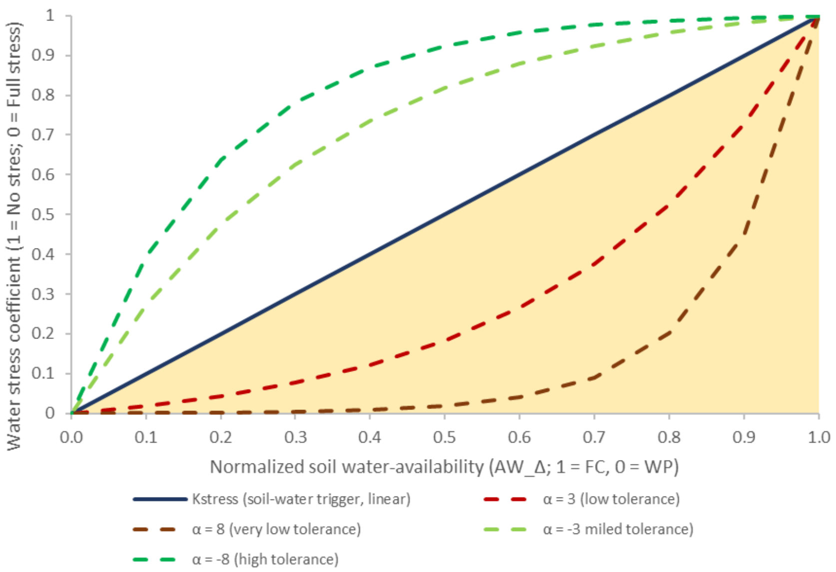

Figure 4. Two-stage water stress cascade in EaSiCroM. The linear Kstress coefficient (solid blue line) represents the soil-water availability trigger; the non-linear KScc coefficient (dashed curves, for various values of shape parameter α) is derived from Kstress.

2.6. Stress-Adjusted Canopy Development

Starting from the potential LAI trajectory of Equation (3), daily canopy expansion is simultaneously constrained by water and temperature stress. The daily increment of the stress-adjusted LAI is:

$$\Delta LAI_{adj} = (LAI_t\text{-}LAI_{t-1})\cdot KS_{cc}\cdot Tlim \tag{13}$$

The cumulative stress-adjusted LAI is then updated as:

$$\begin{cases} LAI_{adj,cumt} = LAI_{adj,cumt-1} \quad \text{if } \Delta LAI_{adj} < 0 \\ \qquad\qquad \text{otherwise} \\ LAI_{adj,cumt} = LAI_{adj,cumt-1} + \Delta LAI_{adj} \end{cases} \tag{14}$$

The conditional in Equation (14) prevents $LAI_{adj,cum}$ from decreasing during the growth phase: leaf area formed under stressful conditions is conserved until the natural senescence signal from the beta function takes over. The stress-adjusted canopy cover is derived from $LAI_{adj,cum}$ using Equations (4) and (5):

$$CC_{adj} = \max\left(0, \left(1\text{-}e^{-f_{cover}\cdot LAI_{adj,cum}}\right)\cdot CF_{adj}\right) \tag{15}$$

where CF_{adj} is computed from $LAI_{adj,cum}$. CC_{adj} is subsequently used in all downstream modules – transpiration, biomass, soil evaporation, and irrigation decision – ensuring complete internal consistency between canopy state and water fluxes.

2.7. Biomass Accumulation and the CO_2 Fertilisation Effect

Before estimating daily biomass, EaSiCroM pre-computes a dimensionless multiplier Δ_{CO_2} that adjusts the potential daily total dry matter (TDM) upward under elevated CO_2, reflecting enhancement of both water-use efficiency and the photosynthesis (RUE) pathway, using Michaelis-Menten kinetics applied to the CO_2 response of photosynthesis (Figure 5; [31]):

$$GR_{ref} = \frac{V_{CO_2,\max}\cdot[CO_2]_{ref}}{[CO_2]_{ref}+K_M} \tag{16a}$$

$$GR_{act} = \frac{V_{CO_2,\max}\cdot[CO_2]_{act}}{[CO_2]_{act}+K_M} \tag{16b}$$

$$\Delta_{CO_2} = \frac{GR_{act}}{GR_{ref}} \tag{16c}$$

where $V_{CO_2,max}$ is the maximum CO_2-driven growth rate, KM the Michaelis-Menten half-saturation constant (ppm), $[CO_2]_{ref}$ the reference atmospheric CO_2 concentration, and $[CO_2]_{act}$ the actual or projected concentration. $\Delta\ CO_2 \geq 1$ when $[CO_2]_{act} > [CO_2]_{ref}$, scaling WP upward in proportion to the

CO_2 fertilisation effect. Setting $[CO_2]$ref equal to $[CO_2]$act disables the sub-model entirely, returning baseline behaviour.

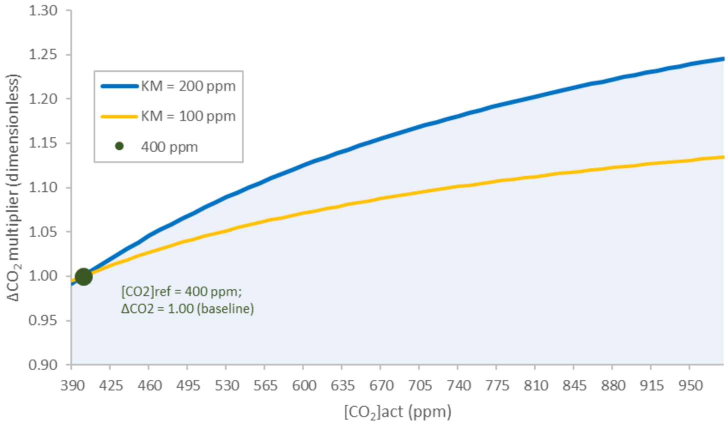

Figure 5. Michaelis–Menten CO_2 fertilisation multiplier Δ CO_2 as a function of actual atmospheric CO_2 concentration $[CO_2]$act, relative to a reference of 400 ppm, for two values of the half-saturation constant KM. The filled circle marks the reference condition (Δ CO_2 = 1.00 at 400 ppm).

The primary approach to daily total dry matter (TDM, kg ha^{-1}) accumulation is based on the concept of water productivity [32,33]:

$$TDM = Tr_{act} \cdot WP \cdot \Delta_{CO_2} \quad (17)$$

where WP (kg mm^{-1}) is the biomass produced per unit of water transpired and Tract is actual crop transpiration:

$$Tr_{act} = K_c \cdot CC_{adj} \cdot ET_0 \quad (18)$$

with Kc the crop coefficient at canopy development [21] and ET_0 reference evapotranspiration. Equation (18) scales potential transpiration demand by the current CC_{adj}, so that early-season and stress-reduced crops consume water proportionally less. When daily solar radiation data Rg (MJ m^{-2} day^{-1}) are available, an alternative biomass estimate based on radiation-use efficiency (RUE, g MJ^{-1} intercepted PAR) is computed:

$$TDM_{RUE} = \frac{CC_{adj} \cdot R_g \cdot 0.48 \cdot RUE}{1000} \cdot 10000 \cdot \Delta_{CO_2} \quad (19)$$

where 0.48 converts total radiation to photosynthetically active radiation [34]. When both approaches are available, the co-limiting minimum rule applies:

$$TDM_{eff} = \min(TDM, TDM_{RUE}) \quad (20)$$

This co-limiting logic prevents systematic overestimation by selecting, on each day, whichever resource – water or radiation – is the most limiting [25]. In the absence of radiation data, TDM_{eff} reverts to the WP-based estimate alone. The sensitivity of simulated TDM trajectories to the degree of crop water stress is illustrated in Figure 6

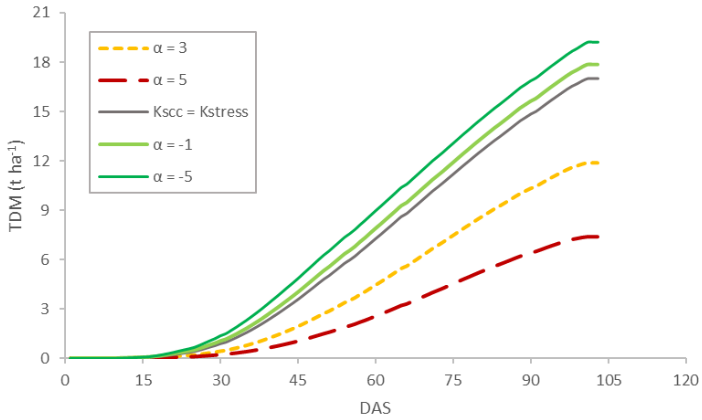

Figure 6. Simulated seasonal trajectories of total dry matter (TDM) for a generic annual crop under four levels of resilience (α) to water stress (Kstress), as simulated by EaSiCroM.

2.8. Stress-Corrected Transpiration and Soil Evaporation

The actual crop water extraction from the soil, Tr_{adj} (mm day^{-1}), applies the linear water stress coefficient to the potential transpiration:

$$Tr_{adj} = K_{stress} \cdot Tr_{act} \tag{21}$$

Tr_{adj} feeds back into the daily soil water balance (Equation 6) as the principal transpiration sink and is tracked cumulatively. Note the distinction between Tr_{act} – the potential canopy-level transpiration used to drive biomass accumulation (Equation 17) – and Tr_{adj} – the actual water extracted from the soil, constrained by Kstress.

Soil evaporation from bare or partially covered soil is estimated using a two-stage model following [21,35], as illustrated in Figure 7. In stage 1 (energy-limited evaporation), the upper limit E_{bs} is driven by ET_0 and controlled by the readily and total evaporable water parameters:

$$E_{\mathrm{bs,t}} = ET_0 \cdot \min\left(\frac{REW}{ET_0}, 0.15 \cdot \frac{TEW\text{-}E_{\mathrm{bs,t-1}}}{TEW\text{-}REW}\right) \tag{22}$$

On the first simulation day, $E_{bs,1}$ = REW / ET_0. In stage 2 (soil-hydraulic-limited), the evaporation reduction coefficient K_{ev} captures the non-linear decline in hydraulic conductivity as the topsoil dries, governed by the texture-dependent shape factor f_k:

$$K_{ev} = \begin{cases} 1 & \text{if AW\_}\Delta\geq 1 \\ \text{otherwise} \\ \frac{e^{f_k \cdot \mathrm{AW\_}\Delta - 1}}{e^{f_k}\text{-}1} \end{cases} \tag{23}$$

The potential evaporation from the exposed soil fraction is then:

$$E_{pot} = K_{ev} \cdot \mathrm{REW} \cdot \left(1\text{-}CC_{adj}\right) \tag{24}$$

and the actual daily evaporation is the minimum of the energy-limited and water-availability-limited bounds:

$$E_{adj} = \min\left(E_{bs}, E_{pot} \cdot f_{vadj}\right) \tag{25}$$

where f_{vadj} is computed as:

$$f_{vadj} = \left(\frac{(REW+1)}{20}\right)^{\frac{1}{n}} \tag{26}$$

where n is a soil-specific shape parameter and f_{vadj} is a soil-surface adjustment factor accommodating the effect of mulch or surface residue on evaporation losses. Total daily crop evapotranspiration is:

$$ET_{\mathrm{c,daily}} = Tr_{adj} + E_{adj} \tag{27}$$

doi:10.20944/preprints202603.1175.v1

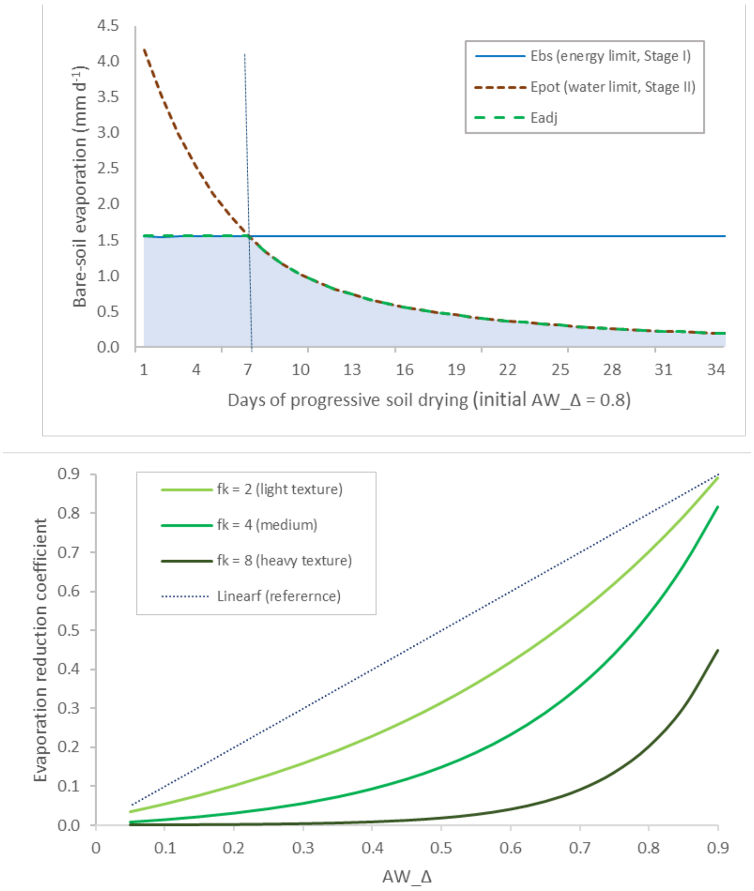

Figure 7. Two-stage bare-soil evaporation model in EaSiCroM (above), simulated over 34 days from an initial soil water availability AW_2 = 0.8, showing energy-limited Stage I (constant E_{bs}) and water-limited Stage II (declining E_{pot} and E_{adj}); and evaporation reduction coefficient K_{ev} as a function of normalised soil-water availability (AW_Δ) for three soil texture classes (light, medium, and heavy), governed by shape parameter f_k.

2.9. Yield Formation

Heat stress during reproductive growth can reduce harvest yields through negative effects on pollen viability, fertilisation, and fruit set, independently of vegetative biomass accumulation [36,37]. EaSiCroM represents this through a separate temperature penalty function on yield:

$$\mathrm{f}(T_{lim,yield}) = \begin{cases} 1 \quad \text{if } T_{mean} < T_{crit,yield} \\ 0 \quad \text{if } T_{mean} > T_{extr,yield} \\ \qquad \text{otherwise} \\ \exp\left(-\lambda \cdot (T_{mean} - T_{crit,yield})\right) \end{cases} \tag{28}$$

where $T_{crit,yield}$ is the temperature above which yield starts to decline, $T_{extr,yield}$ the lethal threshold (zero yield production), and λ controls the steepness of the exponential decline. This function is intentionally decoupled from the vegetative stress factor T_{lim} (Equation 2), allowing different thermal sensitivities to be assigned to the two phases of crop development – a distinction supported by a growing body of evidence showing that pollen tube elongation and fertilisation are among the most heat-sensitive physiological processes in crop plants [36].

Fruit or seed yield accumulates only after a crop-specific thermal threshold $GDD_{start,yield}$ is exceeded, reflecting the lag between canopy establishment and the onset of reproductive sink activity:

$$\begin{cases} Y_{\text{daily}} = TDM_{eff} \cdot \mathrm{HI} \cdot \mathrm{f}(T_{\text{lim,yield}}) \quad \text{if } GDD_{cum} > GDD_{start,yield} \\ \qquad\qquad \text{otherwise} \\ Y_{\text{daily}} = 0 \end{cases} \tag{29}$$

and:

$$Y_{cum,t} = Y_{cum,t-1} + Y_{daily,t} \quad (30)$$

where HI is the harvest index (fraction of total dry matter partitioned to the harvested organ). Both HI and $GDD_{start,yield}$ are crop- and variety-specific parameters. Fresh yield at harvest can be obtained from cumulative dry yield using the user-specified water content of the yield. The sensitivity of $f(T_{lim,yield})$ to the thermal threshold parameters and the steepness coefficient λ is illustrated in Figure 8 for two representative crop types with contrasting heat tolerance.

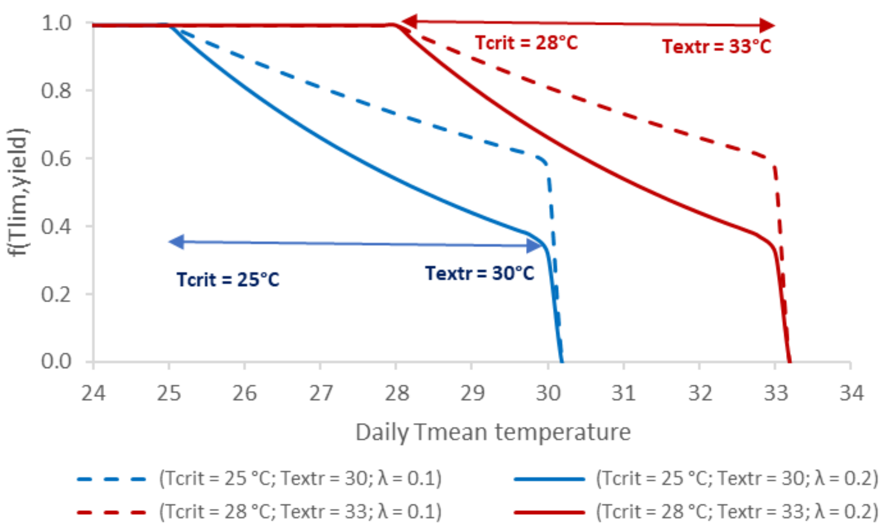

Figure 8. Yield heat-stress penalty function $f(T_{lim,yield})$ as a function of daily mean temperature, for four combinations of the controlling parameters $T_{crit,yield}$, $T_{extr,yield}$, and λ.

2.10. Irrigation Scheduling

EaSiCroM offers three distinct and user-selectable irrigation triggering strategies, all operating within a user-defined irrigation window expressed as a range of days after sowing [DAS_{start}, DAS_{end}]. The water depletion strategy triggers irrigation when the fraction of plant-available water remaining in the root zone falls below a user-specified threshold p_{depl}:

$$IRR = \begin{cases} \max(\theta\Delta - (AWC - \theta_{WP,root}), 0) & \text{if } AWC - \theta_{WP,root} < \theta\Delta \cdot p_{depl} \text{ and } DAS \in [DAS_{start}, DAS_{end}] \\ 0 & \text{otherwise} \end{cases}$$

(31)

The volume supplied refills the root zone to field capacity. A larger value of p_{depl} results in more frequent but smaller irrigation events, while a smaller value triggers irrigation only when depletion is severe. The water consumption strategy instead triggers irrigation when the cumulative volume consumed from the soil ($\theta_{FC,root}$ − AWC) exceeds a user-defined volumetric threshold:

$$IRR = \theta_{FC_{root}} - AWC \text{ if } \theta_{FC_{root}} - AWC > \text{threshold} \quad (32)$$

This approach ties irrigation timing directly to crop water use rather than to a static soil fraction and is particularly suited to crops with strongly variable daily transpiration rates. Finally, the user strategy accepts user-supplied irrigation dates and volumes from an uploaded CSV file:

$$IRR = IRR_{user} \quad (33)$$

For rainfed simulations, the file contains a single date with an irrigation value of zero. In real-time mode, a minimum irrigation threshold (mm) can additionally be specified, below which EaSiCroM will not trigger water application – a practical feature for pivot systems where operators prefer to synchronise irrigation across multiple field sectors rather than respond to individual subplots in isolation.

2.11. Observed Data Assimilation and Forced Canopy States

When user-provided canopy cover (CC), leaf area index (LAI), or total available water (TAW) observations are available (whether from field measurements, remote sensing, or any other source), EaSiCroM can operate in a forced mode in which simulated values are replaced by the observed ones. For CC forcing, the corresponding $LAI_{adj,cum}$ is back-calculated by inverting the Beer-Lambert relationship of Equation (5):

$$\begin{cases} LAI_{\mathrm{adj,cum}} = -\frac{\ln(1-CC)}{f_{cover}} & \text{if CC > CF} \\ \text{otherwise} & \\ LAI_{\mathrm{adj,cum}} = -\frac{\ln\left(\frac{CF-CC}{CF}\right)}{f_{cover}} & \end{cases} \tag{34}$$

and the daily adjusted LAI increment is derived as:

$$\Delta LAI_{adj} = LAI_{adj,cumt} - LAI_{adj,cumt-1} \tag{35}$$

This assimilation mechanism allows the model to correct accumulated simulation errors in canopy development using user-provided observations. Forcing data are provided via a CSV file containing observation dates, subplot IDs, and measured values for CC, LAI, or TAW.

2.12. Multi-Plot Simulation and Real-Time Precision Irrigation

EaSiCroM supports concurrent simulation of multiple plots through a numeric ID system. Each plot can be assigned to its own soil hydraulic properties, crop parameters, and irrigation strategy. This architecture enables three classes of application: (i) monoculture fields with sub-field heterogeneity in soil texture or initial water content, where different IDs share the same crop parameters; (ii) crop rotations in which successive crops are linked to the same field ID across multiple years; and (iii) spatially resolved precision irrigation, where each spatial unit is treated as an independent plot with its own water balance. In multi-simulation mode, weather files are named with the corresponding field ID; for monocultures, each ID corresponds to a specific agricultural year. The harvest date in seasonal output corresponds to the last date in the weather file, while the daily output file records the actual end of the crop cycle at physiological maturity.

In the real-time simulation mode, the system ingests daily updated weather data (or multi-day forecasts) and combines them with subplot-specific forcing files to generate irrigation recommendations for each subplot independently. If an irrigation recommendation coincides with the last day of the available weather file, EaSiCroM prompts the user in the subsequent simulation run to confirm whether irrigation was carried out; if not, the undelivered volume is accumulated and added to the following day's requirement. Should the simulation window extend beyond a day for which irrigation was recommended without user input, delivery is assumed to have taken place. These features collectively make EaSiCroM an adaptive, field-ready tool for variable-rate irrigation management (Figure 9).

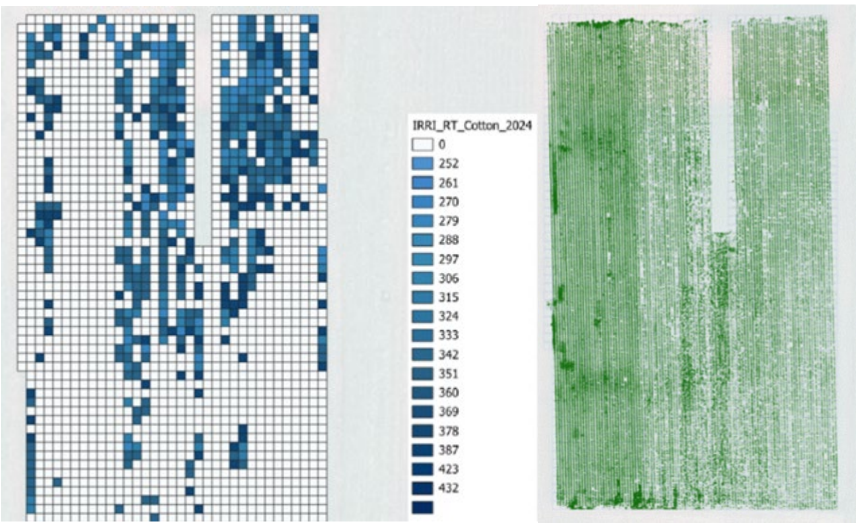

 doi:10.20944/preprints202603.1175.v1

Figure 9. Example of a spatially explicit irrigation prescription map generated by EaSiCroM for a cotton field on a specific mapping date. Left: irrigation requirement map simulated by EaSiCroM through CC assimilation (Equation 35), reflecting the actual crop water demand and phenological state at sub-field resolution. Right: daily canopy cover (CC) map derived from a drone-based remote sensing flight, used as forcing input .

2.13. Software Implementation and Deployment

EaSiCroM is implemented in Python and distributed as a containerised web application. The computational core is encapsulated within a Docker image to ensure platform-independent execution across Windows, macOS, and Linux systems. Containerisation guarantees strict reproducibility by preserving software dependencies and runtime configuration. The graphical interface operates through a standard web browser, while all simulations are executed within the isolated computational environment. The EaSiCroM container image is freely available for download from a public repository (https://drive.google.com/drive/folders/1E0Fq5Hk_4u0xaCV1ilXixGHEfSvWL4aK).

The user interface guides parameter entry for soil, crop, and climate change scenarios, with inline help tooltips for each field (Figure 10). Soft validation alerts the user when input values fall outside model-recommended ranges, while still permitting overrides when site-specific knowledge justifies departures from typical values. Weather data and forcing files are provided in CSV format following the structure distributed with the application. Example input files for single-crop, multiple-simulation, and real-time modes are included.

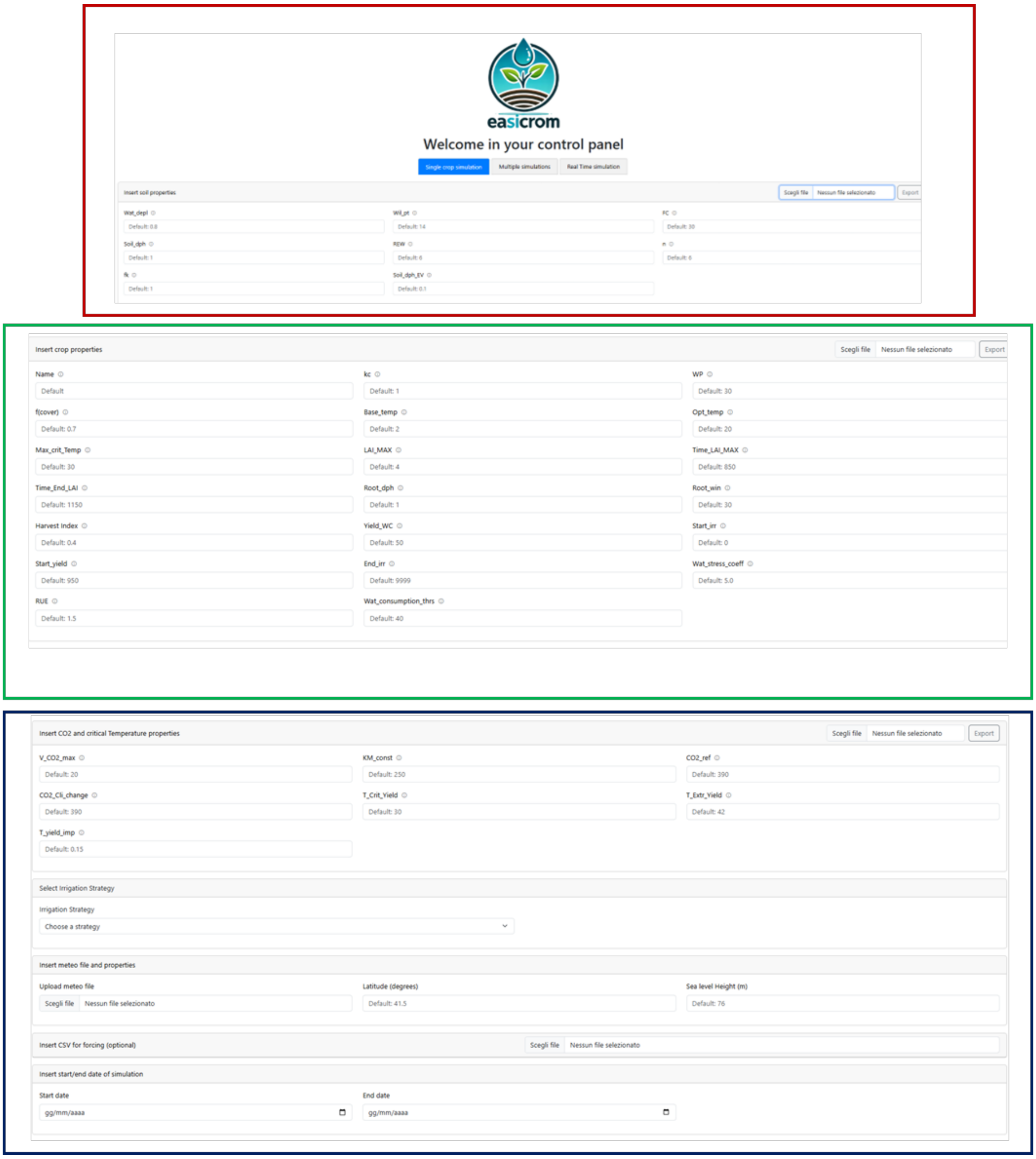

Figure 10. EaSiCroM user interface for single-crop simulations. Coloured boxes indicate the input parameter groups: soil hydraulic properties (red), crop-specific parameters (green), and climate change scenario settings, irrigation strategy, meteorological variable selection, and simulation period (blue).

3. Discussion

The development of EaSiCroM was motivated by a gap that remains persistent in the landscape of crop simulation tools: the relative scarcity of systems that combine sufficient mechanistic depth to simulate crop-environment interactions realistically, with the parsimony and usability demanded by operational irrigation management contexts. The design philosophy deliberately follows the "fit-for-purpose" principle of [38], according to which model complexity should be commensurate with the precision of the available input data and the resolution of the agronomic questions being addressed. In what follows we discuss the principal design decisions and their agronomic implications, compare EaSiCroM with existing tools, and identify residual limitations and prospects for future development.

The choice of empirical growth functions — the beta function for LAI and the WP-based approach for biomass accumulation — reflects an explicit preference for robustness and transparency over mechanistic completeness. The beta function requires only three parameters (LAI_{max},

Preprints.org (www.preprints.org) | NOT PEER-REVIEWED | Posted: 16 March 2026 doi:10.20944/preprints202603.1175.v1

$GDDLAI_{max}$, GDD_{end}), each with a clear physiological interpretation and direct observational counterpart. It reproduces the asymmetric trajectory of annual crop canopies — rapid establishment, a plateau near maximum leaf area, and gradual senescence — across a wide range of species and environments without sub-stage parameterisation [27]. More elaborate formalisms, such as the organ-level growth models embedded in DSSAT [12] or APSIM [13], provide greater mechanistic detail but require extensive calibration datasets that are rarely available in operational contexts. The beta function thus represents a pragmatic optimum between realism and parsimony.

The parsimony of EaSiCroM is most evident when the parameter requirements are placed in direct comparison with those of existing frameworks. EaSiCroM requires approximately 25 crop- and soil-specific parameters in total (including thermal thresholds, canopy descriptors, water productivity, harvest index, and soil hydraulic properties), all of which carry a clear physiological meaning and can be estimated from standard agronomic experiments or published literature. In contrast, DSSAT [12] typically requires upwards of 50–80 genotype-specific and ecotype coefficients per crop, while APSIM [13] demands comparable or greater numbers across its soil, plant, and management modules. AquaCrop [14], which shares a similar WP-based philosophy, requires approximately 30 parameters but lacks the canopy data assimilation, real-time and multi-plot architecture, present in EaSiCroM. Even simpler tools such as FAO-56 [21], while requiring very few inputs, do not simulate dynamic canopy development, biomass, or yield, and thus cannot support the level of decision-making detail that precision irrigation management demands. The deliberately minimal parameter set of EaSiCroM therefore constitutes not merely a convenience but a design principle: reducing the calibration burden directly extends the operational reach of the system to practitioners and irrigation advisors who lack access to detailed experimental datasets.

One of the most agronomically important design decisions in EaSiCroM is the separation of the canopy expansion stress coefficient KScc (Equation 12) from the soil-water availability indicator Kstress (Equation 11). This distinction is grounded in well-established plant physiology: turgor-driven leaf expansion is typically more sensitive to water deficit than stomatal conductance and gas exchange, so leaf area begins to decline at higher soil water contents than does transpiration [28,29]. Representing this differential sensitivity with a single, unified stress coefficient — as many simpler models do — inevitably introduces systematic biases in either canopy development or water use, particularly under mild to moderate deficit irrigation strategies that deliberately exploit crop tolerance to sub-optimal water supply. The non-linear KScc function with its shape parameter α provides a flexible, physiologically interpretable instrument for tuning this differential sensitivity to the characteristics of the specific crop and irrigation regime. AquaCrop [14] adopts a conceptually analogous approach with separate expansion and transpiration stress coefficients, lending additional validation to the dual-coefficient architecture.

The water productivity (WP) approach to biomass accumulation follows the transpiration efficiency framework of [32]. In EaSiCroM, WP is a crop-specific parameter provided by the user (expressed in kg dry matter per mm of transpiration); it represents a species-level constant calibrated from experimental data or published values. This approach has been validated across dozens of crop species and climatic environments worldwide [33]. Its central advantage is the relative conservativeness of WP: for a given species it varies little across sites and seasons, making it a stable and reliable calibration target estimate from a relatively small experimental dataset. The optional RUE co-limiting pathway (Equation 18) extends this approach to situations where solar radiation data are available, providing a more balanced representation of growth limitation by both water and light — a scheme whose agronomic rationale was demonstrated for biomass sorghum in a Mediterranean environment by [25] and which applies analogously across annual crop species. The co-limiting minimum rule prevents systematic overestimation that would result from applying either the WP or the RUE estimate alone in all conditions.

The Michaelis-Menten CO_2 fertilisation sub-model (Equations 16a–16c) constitutes a novel feature that distinguishes EaSiCroM from most operational IDSSs currently in use. Atmospheric CO_2 concentrations have now surpassed 425 ppm and are projected to exceed 500 ppm under intermediate

 doi:10.20944/preprints202603.1175.v1

emission scenarios by mid-century [8], implying a non-trivial fertilisation effect on the water-use efficiency of C3 crops: meta-analyses of free-air CO_2 enrichment (FACE) experiments indicate mean yield increases of approximately 12–17% at 550 ppm relative to ambient conditions, primarily through increased photosynthetic rate and reduced stomatal conductance [39,40]. Ignoring this effect leads to a systematic underestimation of actual WP and hence of biomass and yield under future climatic conditions. The Michaelis-Menten formulation produces a saturating CO_2response consistent with Free-Air CO_2Enrichment (FACE) experiments and controlled-environment studies demonstrating asymptotic increases in photosynthetic assimilation and water productivity under elevated CO_2 concentrations [31,41]. Computationally, ΔCO_2 is pre-computed once during model initialization and applied as a constant daily multiplier, adding negligible overhead to the simulation. Users who wish to simulate baseline conditions without CO_2 enrichment effects need only set the reference and actual CO_2 concentrations to the same value.

The two-stage soil evaporation model (Equations 22–25) represents a clear advance over the single-coefficient approaches that characterize many simpler IDSSs. By explicitly tracking the progressive depletion of a finite topsoil pool of readily evaporable water (REW), the model correctly reproduces the characteristic pattern of bare-soil evaporation: high rates the period immediately after irrigation or rainfall while the soil surface is wet (stage 1, energy-limited), followed by a rapid decline as the surface layer dries and hydraulic conductivity decreases (stage 2, water-limited). This behaviour is particularly consequential in Mediterranean climates, where irrigation events are often spaced several days apart and bare-soil evaporation between events can represent a substantial fraction of total water loss. The interaction between E_{bs} (energy limit) and E_{pot} (water availability limit) through the minimum function in Equation (25) ensures that neither constraint alone can drive evaporation beyond what both simultaneously permit. The f_{vadj} parameter provides an additional degree of calibration flexibility to account for the dampening effect of mulch, crop residue, or surface crust on evaporative losses.

The introduction of a separate heat-stress function $f(T_{lim,yield})$ specifically for reproductive growth (Equation 28) reflects a growing body of evidence showing that the reproductive phase is substantially more sensitive to high temperatures than vegetative biomass accumulation [36,37]. Decoupling the thermal responses of vegetative and reproductive processes allows EaSiCroM to simulate agronomically realistic scenarios in which brief, intense heat waves during anthesis and fruit formation cause disproportionate yield losses relative to the apparent impact on total seasonal biomass — a pattern increasingly documented for wheat, maize, and tomato under Mediterranean summer conditions [36]. The exponential decline in $f(T_{lim,yield})$ provides a smooth, physiologically plausible function in which the steepness parameter λ can be adjusted to match the known heat sensitivity of the specific crop variety.

The observed data assimilation capability (Section 2.11) represents the most architecturally innovative feature with respect to earlier versions of this modelling framework. Allowing users to supply observed canopy or soil-water data from any source — field measurements, remote sensing, or sensor networks — enables EaSiCroM to correct its internal state and generate spatially differentiated irrigation prescriptions that reflect genuine intra-field heterogeneity in crop development. This positions EaSiCroM within the emerging paradigm of agriculture digital twins — continuously updated virtual representations of cropped fields that assimilate observational data streams to improve decision support [23]. In the real-time precision irrigation mode, the minimum intervention threshold further adds a layer of operational intelligence that aligns the model's recommendations with the practical constraints of specific irrigation delivery systems, such as pivots that must move across an entire field rather than irrigate individual subplots in isolation.

The choice of Docker as the deployment platform directly addresses one of the most persistent and underappreciated barriers to IDSS adoption in practice: software installation complexity and dependency conflicts across diverse computing environments. A survey of public IDSSs in Italy by [11] highlighted that ease of installation and accessibility were among the principal factors determining uptake by farmers and irrigation advisors — more so, in many cases, than scientific

Preprints.org (www.preprints.org) | NOT PEER-REVIEWED | Posted: 16 March 2026 doi:10.20944/preprints202603.1175.v1

sophistication. All dependencies (Python interpreter, numerical libraries, web framework, and auxiliary modules) are encapsulated within a fixed runtime environment. This eliminates variability arising from local system configuration, library version conflicts, or operating system differences. In the context of scientific modelling and decision support systems, reproducibility is not a secondary concern but a fundamental requirement for transparency and peer verification. The web-browser interface operates exclusively as a front-end layer, while all numerical computations remain unchanged regardless of the client platform. This separation between computational core and interface ensures methodological stability across deployments.

Compared to mechanistically rich models such as DSSAT or APSIM, EaSiCroM sacrifices explicit representation of nitrogen cycling, root architecture dynamics, and pest-disease interactions. For situations where these processes are the primary subject of analysis, full process-based models remain the appropriate choice. In EaSiCroM, the effective root-zone depth is treated as a user-defined constant during the simulation cycle. This simplification reflects a deliberate modelling boundary: the framework is intended for operational irrigation scheduling once the maximum effective rooting depth of the crop under local soil conditions has been established. For annual crops grown under conventional management, root systems typically reach a quasi-stationary effective depth well before peak water demand. Within this operational context, dynamic root growth modelling adds parameter uncertainty without proportionate gains in irrigation accuracy. Consequently, EaSiCroM assumes that the active soil layer contributing to transpiration has been characterised a priori and remains constant for the purposes of daily water balance computation.

EaSiCroM does not solve the Richards equation nor simulate vertical water flux within layered soil profiles. Instead, the soil compartment is represented by bulk hydraulic parameters defined over the effective root zone: volumetric water content at field capacity (θ_{FC}), volumetric water content at permanent wilting point (θ_{WP}), and the derived plant-available water (PAW). No explicit bulk density parameter is required, as water content is expressed on a volumetric basis and soil structural effects are implicitly embedded in the calibrated θ_{FC} and θ_{WP} values. This lumped representation is adequate for daily root-zone water balance and irrigation scheduling, but it is not intended for detailed infiltration dynamics or deep percolation analysis. The modelling philosophy is therefore consistent with a bucket-type water balance abstraction rather than a mechanistic soil physics simulator.

However, for the specific application domain of irrigation scheduling and water-resource management in annual crops, the present level of complexity is judged sufficient and appropriate — and the simplifications are explicitly acknowledged rather than concealed behind a cost of agronomic accuracy.

Compared to simpler FAO-56-type water balance tools, EaSiCroM provides substantially richer information: dynamic canopy cover and LAI, daily partitioning of transpiration and soil evaporation, stress-adjusted biomass and yield, spatial variability handling through multi-plot simulation, long-term scenario analyses with changing CO_2, and adaptive real-time scheduling. These features collectively position EaSiCroM as a more informative and flexible tool for irrigation practitioners, water-resource managers, and agricultural researchers. A comparative overview of selected features of EaSiCroM against two widely used crop modelling frameworks is provided in Table 1.

Table 1. Comparative overview of selected features of EaSiCroM, AquaCrop, and FAO-56.

Feature	EaSiCroM	AquaCrop	FAO-56
Canopy model	Beta-function LAI + Beer-Lambert CC	Canopy cover (CC) dynamic	Crop coefficient Kc
Time step	Daily	Daily	Daily

Feature	EaSiCroM	AquaCrop	FAO-56
Biomass / yield	WP + optional RUE; HI-based yield	WP-based; HI yield	Not simulated
Soil water balance	Root-zone bucket; drainage	Root-zone bucket; drainage	Root-zone bucket
Water stress	Dual: Kstress (linear) + KScc (non-linear)	Multiple: Ks for canopy development, stomatal closure and anticipated senescence	Single Ks coefficient
CO_2 fertilisation	Yes — Michaelis–Menten sub-model	Yes — WP scaling	No
Bare-soil evaporation	Yes — two-stage (REW/TEW)	Yes — two-stage	Yes — dual Kcb/Ke
Reproductive heat stress	Yes — explicit yield penalty function	Yes	No
Canopy data assimilation	Yes — CC, LAI, TAW forcing	No	No
Multi-plot simulation	Yes — numeric ID system	Limited	No
Deployment	Docker web app	Desktop GUI / web	Spreadsheet / manual
Freely available	Yes — container image	Yes — open source	Yes — guidelines only

4. Conclusions

This paper has presented the mathematical foundations, architectural design, and software deployment of EaSiCroM – the Easy Simulator Crop Model – a modular, low-parameterisation decision support system for crop growth simulation and irrigation management. EaSiCroM integrates canopy development, soil water balance, transpiration, biomass accumulation, soil evaporation, and yield formation in a coherent, hierarchically ordered daily simulation framework in which all major growth-limiting factors – temperature stress, water stress, CO_2 fertilisation, and reproductive heat stress – are explicitly and consistently represented.

Its principal strength lies in the combination of parsimony – a limited and clearly interpretable parameter set estimable from standard agronomic data – with genuine mechanistic depth: the dual water stress coefficient architecture replicates the differential drought sensitivity of canopy expansion versus transpiration; the Michaelis-Menten CO_2 sub-model provides a theoretically grounded account of future fertilisation effects; the two-stage evaporation model correctly captures post-irrigation surface drying dynamics; and the separate reproductive heat stress function allows realistic simulation of yield responses to short heat waves during anthesis. The observed data assimilation mechanism and multi-plot concurrent simulation framework enable spatially resolved, adaptive irrigation prescriptions at sub-field resolution, while the Docker containerisation and browser interface make the system accessible to a broad range of users without installation complexity.

EaSiCroM is freely available to the scientific community and to practitioners as a ready-to-run containerised application, with the goal of supporting the dissemination of sustainable, data-informed irrigation management in water-scarce agricultural regions worldwide. Experimental validation across multiple crops and environments, together with future model extensions, will be the subject of subsequent contributions.

5. Patents

The EaSiCroM software (Easy Simulation Crop Model) has been registered in the Italian Public Special Register for Computer Programs maintained by SIAE — Società Italiana degli Autori ed Editori (Italian Society of Authors and Publishers), pursuant to Articles 2 and 3 of DPCM No. 244/1994. Registration number: D000025126; progressive number: D000026550; deposit date: 20 February 2025.

Author Contributions: Conceptualization, P.G.; Methodology, P.G.; Software, L.M., S.R. and D.I.; Formal Analysis, P.G and M.R.; Writing — Original Draft Preparation, P.G.; Writing — Review & Editing, P.G., M.R., D.I., L.M., F.C. and S.R.; Visualization, P.G; Resources: S.R. All authors have read and agreed to the published version of the manuscript.

Funding: This research received no external funding.

Data Availability Statement: The EaSiCroM container image and example input files are freely available for download from the following public repository: https://drive.google.com/drive/folders/1E0Fq5Hk_4u0xaCV1ilXixGHEfSvWL4aK.

Conflicts of Interest: The authors declare no conflicts of interest.

References

1. FAO. The State of Food and Agriculture 2020. Overcoming Water Challenges in Agriculture. FAO, Rome, 2020.
2. Rockström, J.; Falkenmark, M.; Karlberg, L.; et al. Future water availability for global food production: The potential of green water for increasing resilience to global change. Water Resources Research 2009, 45, W00A12.
3. Giorgi, F.; Lionello, P. Climate change projections for the Mediterranean region. Global and Planetary Change 2008, 63, 90–104.
4. Kang, Y.; Khan, S.; Ma, X. Climate change impacts on crop yield, crop water productivity and food security – A review. Progress in Natural Science 2009, 19, 1665–1674.
5. ISTAT. Il censimento delle acque per uso civile. Istituto Nazionale di Statistica, Rome, 2019. (https://www.istat.it/informazioni-sulla-rilevazione/cens-acque/. (Last access, March 2026)
6. Tilman, D.; Balzer, C.; Hill, J.; Befort, B.L. Global food demand and the sustainable intensification of agriculture. Proceedings of the National Academy of Sciences 2011, 108, 20260–20264.
7. Arora, N.K. Impact of climate change on agriculture production and its sustainable solutions. Environmental Sustainability 2019, 2, 95–96.
8. IPCC. Climate Change 2022: Impacts, Adaptation and Vulnerability. Contribution of Working Group II to the Sixth Assessment Report. Cambridge University Press, Cambridge, 2022.
9. UN. Transforming Our World: The 2030 Agenda for Sustainable Development. Resolution A/RES/70/1. United Nations, New York, 2015.
10. Rinaldi, M.; He, Z. Decision Support Systems to Manage Irrigation in Agriculture. Advances in Agronomy 2014, 123, 229–280.

11. Sportelli, M.; Crivello, A.; Bacco, M.; Rallo, G.; Brunori, G. Public irrigation decision support systems (IDSS) in Italy: Description, evaluation and national context overview. Smart Agricultural Technology 2024, 9, 100564.
12. Jones, J.W.; Hoogenboom, G.; Porter, C.H.; et al. The DSSAT cropping system model. European Journal of Agronomy 2003, 18, 235–265.
13. Holzworth, D.P.; Huth, N.I.; deVoil, P.G.; et al. APSIM – Evolution towards a new generation of agricultural systems simulation. Environmental Modelling & Software 2014, 62, 327–350.
14. Steduto, P.; Hsiao, T.C.; Raes, D.; Fereres, E. AquaCrop – The FAO crop model to simulate yield response to water: I. Concepts and underlying principles. Agronomy Journal 2009, 101, 426–437.
15. Stöckle, C.O.; Donatelli, M.; Nelson, R. CropSyst, a cropping systems simulation model. European Journal of Agronomy 2003, 18, 289–307.
16. Ahuja, L.R.; Rojas, K.W.; Hanson, J.D.; Shaffer, M.J.; Ma, L. Root Zone Water Quality Model: Modelling Management Effects on Water Quality and Crop Production. Water Resources Publications, Highlands Ranch, CO, 2000.
17. Leenhardt, D.; Trouvat, J. L; Gonzalès, G.; Pérarnaud, V.; Prats, S.; Bergez, J. E. Estimating irrigation demand for water management on a regional scale: I. ADEAUMIS, a simulation platform based on bio-decisional modelling and spatial information. Agricultural Water Management,2004, 68(3), 207-232.
18. Leenhardt, D.; Trouvat, J. L; Gonzalès, G.; Pérarnaud, V.; Prats, S.; Bergez, J. E. Estimating irrigation demand for water management on a regional scale: II. Validation of ADEAUMIS. Agricultural Water Management 2004, 68(3), 233-250.
19. Pedras, C.M.G.; Pereira, L.S.; Chambel-Leitão, P. MIRRIG: A decision support system for design and evaluation of microirrigation systems. Agricultural Water Management 2009, 96, 691–701.
20. Giusti, E.; Marsili-Libelli, S. A fuzzy decision support system for irrigation and water conservation in agriculture. Environmental Modelling & Software 2015, 63, 73–86.
21. Allen, R.G.; Pereira, L.S.; Raes, D.; Smith, M. Crop Evapotranspiration – Guidelines for Computing Crop Water Requirements. FAO Irrigation and Drainage Paper No. 56. FAO, Rome, 1998.
22. Zucaro, R.; Baralla, S.; Arzeni, A.; et al. Integrating Irrigation Decision Support Systems for Efficient Water Use: A Case Study on Mediterranean Agriculture. Land 2025, 14, 5.
23. Ahmad, U.; Sohel, F. Evaluating Decision Support Systems for Precision Irrigation and Water Use Efficiency. Digital Engineering 2025, 4, 100038.
24. Garofalo, P.; Rinaldi, M. Leaf gas exchange and radiation use efficiency of sunflower (Helianthus annuus L.) in response to different deficit irrigation strategies: From solar radiation to plant growth analysis. European Journal of Agronomy, 2015, 64, 88-97.
25. Garofalo, P.; Ventrella, D.; Mastrorilli, M.; Palumbo, A.D.; Campi, P. An empirical framework for modelling transpiration use efficiency and radiation use efficiency of biomass sorghum in Mediterranean environment. Italian Journal of Agronomy 2020, 15, 49–62.
26. Soltani, A.; Sinclair, T.R. Modeling Physiology of Crop Development, Growth and Yield. CABI, Wallingford, UK, 2012.
27. Yin, X.; Goudriaan, J.; Lantinga, E.A.; Vos, J.; Spiertz, H.J. A flexible sigmoid function of determinate growth. Annals of Botany 2003, 91, 361–371.
28. Hsiao, T.C. Plant responses to water stress. Annual Review of Plant Physiology 1973, 24, 519–570.
29. Tardieu, F.; Simonneau, T.; Muller, B. The physiological basis of drought tolerance in crop plants: a scenario-dependent probabilistic approach. Annual Review of Plant Biology 2018, 69, 733–759.
30. Hsiao, T.C.; Acevedo, E.; Fereres, E.; Henderson, D.W. Water stress, growth, and osmotic adjustment. Philosophical Transactions of the Royal Society B 1976, 273, 479–500.
31. Farquhar, G.D.; von Caemmerer, S.; Berry, J.A. A biochemical model of photosynthetic CO_2 assimilation in leaves of C3 species. Planta 1980, 149, 78–90.
32. Tanner, C.B.; Sinclair, T.R. Efficient water use in crop production: Research or re-search? In: Taylor, H.M. et al. (Eds.), Limitations to Efficient Water Use in Crop Production. American Society of Agronomy, Madison, WI, 1983, pp. 1–27.

doi:10.20944/preprints202603.1175.v1

33. Steduto, P.; Hsiao, T.C.; Fereres, E. On the conservative behavior of biomass water productivity. Irrigation Science 2007, 25, 189–207.
34. McCree, K.J. The action spectrum, absorptance and quantum yield of photosynthesis in crop plants. Agricultural Meteorology 1971, 9, 191–216.
35. Ritchie, J.T. Model for predicting evaporation from a row crop with incomplete cover. Water Resources Research 1972, 8, 1204–1213.
36. Lobell, D.B.; Schlenker, W.; Costa-Roberts, J. Climate trends and global crop production since 1980. Science 2011, 333, 616–620.
37. Hatfield, J.L.; Prueger, J.H. Temperature extremes: Effect on plant growth and development. Weather and Climate Extremes 2015, 10, 4–10.
38. Sinclair, T.R.; Seligman, N. Criteria for publishing papers on crop modeling. Field Crops Research 2000, 68, 165–172.
39. Ainsworth, E.A.; Long, S.P. What have we learned from 15 years of free-air CO_2 enrichment (FACE)? A meta-analytic review of the responses of photosynthesis, canopy properties and plant production to rising CO_2. New Phytologist 2005, 165, 351–372.
40. Long, S.P.; Ainsworth, E.A.; Leakey, A.D.B.; Nösberger, J.; Ort, D.R. Food for thought: lower-than-expected crop yield stimulation with rising CO_2 concentrations. Science 2006, 312, 1918–1921.
41. Kimball, B.A. Crop responses to elevated CO_2 and interactions with H_2O, N, and temperature. Current Opinion in Plant Biology 2016, 31, 36–42.